

Nontrivial causal structures engendered by knotted solitons

E. Goulart*

*CAPES Foundation, Ministry of Education, Brasília, Distrito Federal 70.040-020, Brazil
and Department of Applied Mathematics and Theoretical Physics,
University of Cambridge, Cambridge CB3 0WA, United Kingdom*

(Received 10 November 2014; published 23 February 2015)

It is shown that the causal structure associated to stringlike solutions of the Faddeev-Niemi model is described by an effective metric. Remarkably, the surfaces characterizing the causal replacement depend on the energy momentum tensor of the background soliton and carry implicitly a topological invariant $\pi_3(\mathbb{S}^2)$. As a consequence, it follows that the preimage curves in \mathbb{R}^3 nontrivially define directions where the cones remain unchanged. We expect that these early results may be of importance in understanding time dependent solutions (collisions/scatterings) numerically or analytically.

DOI: 10.1103/PhysRevD.91.045033

PACS numbers: 11.27.+d, 02.40.-k, 04.20.Cv, 11.10.-z

I. INTRODUCTION

The existence of closed stringlike solutions in $(3+1)$ -dimensional field theories is certainly one of the intriguing aspects of modern mathematical physics. Typically, these localized solutions describe one-dimensional structures which may twist nontrivially in the forms of loops, links and knots characterized by a Hopf index. Roughly, a Hopf soliton (or hopfion) is a knot in a three-dimensional continuous unit vector field which cannot be unknotted without cutting [1]. Remarkably, they appear in a variety of physical systems such as Bose-Einstein condensates [2], ferromagnetism [3], magnetohydrodynamics [4] and non-Abelian gauge theories, where they are supposed to describe glueballs [5]. More recently, it was proposed that liquid crystals also provide an ideal setting for exploring such topological phenomena [6].¹

One of the simplest relativistic systems supporting knots is the $O(3)$ variant of the Skyrme model [8]. The so-called Faddeev-Niemi (FN) model describes the dynamics of a three-dimensional isovector $\mathbf{n}(x^a)$ taking values on a bi-dimensional sphere \mathbb{S}^2 i.e. $\mathbf{n} \cdot \mathbf{n} = 1$ [5]. The Lagrangian is that of a sigma model plus fourth order corrections and the topological content appears when we consider static solutions with asymptotic behavior $\mathbf{n}|_\infty = (0, 0, 1)$. In this situation the field realizes the map between spheres $\mathbb{R}^3 \cup \{\infty\} \cong \mathbb{S}^3 \rightarrow \mathbb{S}^2$ which is characterized by the Hopf index. Interestingly, the FN model appears quite naturally in the dual superconducting picture of the strongly coupled $SU(2)$ Yang-Mills theory discussed in a series of papers [9–13]. Accordingly, the high energy limit of the theory may describe asymptotically free, massless pointlike gluons while the infrared limit may describe extended flux tubes which close on themselves in stable knotted

configurations. This scenario is particularly compelling because it is consistent with the accepted notion of color confinement in QCD and therefore can shed some light into the mass gap problem. Unfortunately, the equations are highly nonlinear and most of the results rely on numerical lattice approaches and/or approximations [14–17].

Although important results on the global existence and development of singularities have been obtained for semilinear wave maps (see, for instance, [18–20] and references therein), much less is known about the evolutionary properties of the FN equations. Generically, one expects that not all initial data will be mathematically admissible since for a large class of them the Cauchy problem would be ill-posed. Indeed, it is quite common that quasilinear partial differential equation's (PDE) generate systems which are not of evolutionary type (for some data) even if the theory is Lorentz invariant by construction (see, for instance, [21]). Needless to say, this lack of hyperbolicity may be of crucial importance in numerical simulations where imprecisions in the initial data may originate instabilities, singularities and discontinuous solutions.

In this paper we investigate the causal structure of the FN model and clarify some aspects related to its propagation features. We show that the high frequency excitations on top of background solutions are described by characteristic surfaces governed by a curved effective geometry (see [22] for a review). This is related to the fact that for quasilinear equations wave velocities are not given *a priori*, but change as functions of initial data, directions of propagation and wave polarization. With respect to the new geometry, rays are equivalent to null geodesics, and therefore can be described using traditional tools of general relativity (see [23] for a similar analysis in the context of hydrodynamics). In particular, we show that the causal replacement inherits the Hopf charge of the soliton. In this sense, the present work is a natural generalization of previous results sketched by Gibbons and the author in [24].

*egoulart@cbpf.br

¹See also [7] for a discussion in the context of steady Euler flows.

II. FADDEEV-NIEMI MODEL

A. Kinematics

Formally, the FN model is a Lorentz invariant Lagrangian theory of maps into a surface [19]. It can be implemented in terms of a continuous and surjective map $\phi: (\mathbb{R}^{1+3}, \eta) \rightarrow (\mathbb{S}^2, h)$ where $\eta_{ab} = \text{diag}(+ - - -)$ and $h_{AB}(\phi)$ is the Riemannian metric on the unit 2-sphere. The map induces the pull-back spacetime tensors ϕ^*h and $\phi^*\epsilon$:

$$\begin{aligned} L_{ab} &= h_{AB}(\phi) \partial_a \phi^A \partial_b \phi^B, \\ F_{ab} &= \epsilon_{AB}(\phi) \partial_a \phi^A \partial_b \phi^B, \end{aligned}$$

with ϵ_{AB} the area 2-form on the sphere. Following [25] we call the tensor $\eta^{-1} \circ \phi^*h$ the strain for the map ϕ . The antisymmetric object F_{ab} and the strain satisfy the algebraic relation

$$F^a{}_c F^{cb} = L^a{}_c L^{cb} - L^c{}_c L^{ab}. \quad (1)$$

Typically, one is interested in particular mappings with the asymptotic behavior $\phi^A|_\infty \rightarrow \text{const}$, which means that the state of the fields are homogeneous as they approach spatial infinity.² As usual, we choose this constant such that the field state corresponds to the north pole **N** on the target. Under this boundary condition, $\phi^A(x^0, x^i)$ effectively maps \mathbb{S}^3 in \mathbb{S}^2 for a given time coordinate x^0 and therefore there is a homotopy invariant $Q = \pi_3(\mathbb{S}^2) \in \mathbb{Z}$. Roughly, it will remain the same under any smooth deformation of the map.

According to the above construction the 2-form F_{ab} identically satisfies

$$\partial_b F^{ab} = 0, \quad (2)$$

with $F_{ab}^* \equiv \eta_{abcd} F^{cd}/2$ the dual and η_{abcd} the usual Levi-Civita tensor. Thus, $\exists C_a$ such that $F_{ab} = \partial_{[a} C_{b]}$ everywhere. Also, due to rank considerations, it follows the algebraic relation

$$F_{ab}^* F^{ab} = 0, \quad (3)$$

which leads to a conserved current of the form $J^a = F_{ab}^* C^b$. Whitehead first showed [26] that it is possible to express the Hopf invariant as an integral of the form

$$Q \propto \int_{\mathbb{R}^3} F_{ab}^* C^a t^b dv, \quad (4)$$

with t^b a normalized timelike vector ($t^a t_a = 1$) orthogonal to the space slices and dv the element of volume. Interestingly, the preimage $\phi^{-1}(P)$ of a given point $P \in \mathbb{S}^2$ is an integral

²This is related to the requirement of finiteness of the energy for static configurations.

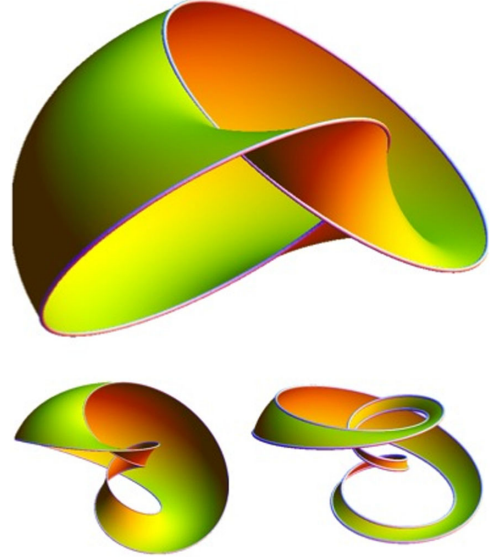


FIG. 1 (color online). Pencils of magnetic field lines in \mathbb{R}^3 for $Q = 1, 2$ and 3 , respectively. The closed curves representing the boundaries of the (Seifert) surfaces correspond to the preimages $\phi^{-1}(P_1)$ and $\phi^{-1}(P_2)$ of two points P_1 and P_2 in \mathbb{S}^2 .

line of the divergenceless magneticlike vector field in \mathbb{R}^3 given by

$$B^a \equiv F^{*a}{}_b t^b. \quad (5)$$

As is well known, Q can be interpreted heuristically as the linking number between two such “magnetic” field lines, $[\phi^{-1}(P_1)]$ and $[\phi^{-1}(P_2)]$, respectively. Generically, these field lines will twist among themselves in a highly nontrivial way for large values of the index, filling the space with a complex fibered structure (see Fig. 1). In particular, the preimage of the south pole **S** is defined as the position of the Hopf soliton as it corresponds to the position in \mathbb{S}^2 more distant to the vacuum.

B. Dynamics

The pulled-back tensors L_{ab} and F_{ab} give rise to invariants from which we can naturally define an action for the map. In the model proposed by Faddeev and Niemi the action is given by

$$S[\phi] = \int \frac{1}{2} L^a{}_a - \frac{\kappa^2}{4} F_{ab} F^{ab} d^4x, \quad (6)$$

where, as usual, the second term (Skyrme term) is introduced to guarantee the stability of solitons against scalings and κ is a parameter controlling the strength of nonlinearities. We note that this term resembles the Lagrangian of Maxwell’s electrodynamics.³

³When one considers static configurations, the first term corresponds to a Dirichlet term and the second to the energy of the vector field B^a directed along the fibers [7].

Variation with respect to ϕ^A yields a system of second order quasilinear PDE's which can be written in the compact form

$$(H_{AB}\partial^a\phi^B)_{||C}\partial_a\phi^C = 0, \quad (7)$$

where

$$H_{AB} \equiv h_{AB} - \kappa^2 \epsilon_{AP} \epsilon_{BQ} X^{PQ}, \quad (8)$$

$X^{AB} \equiv \partial_a \phi^A \partial_b \phi^B \eta^{ab}$ and $||$ represents the covariant derivative with respect to h_{AB} .⁴ In terms of the target connection Γ^A_{BC} , Eq. (7) becomes

$$\partial_a(H_{AB}\partial^a\phi^B) = \Gamma^D_{AC}H_{DB}\partial^a\phi^B\partial_a\phi^C, \quad (9)$$

which reveals that the equation of motion consists of various types of self-interactions arising from the non-standard kinetic terms and the target space geometry.

Generically, it is possible to express Eq. (9) as

$$M^{ab}_{AB}(\phi, \partial\phi)\partial_a\partial_b\phi^B + \dots = 0, \quad (10)$$

where “ \dots ” stands for semilinear terms in ϕ^A (lower order derivatives) and the principal symbol is given by

$$\mathbf{M} = \eta^{ab}H_{AB} + \frac{\kappa^2}{2}\epsilon_{AP}\epsilon_{BQ}\partial^a\phi^Q\partial^b\phi^P. \quad (11)$$

As it is well known, the highest-order terms in derivatives almost completely control the qualitative behavior of solutions of a partial differential equation. We note that \mathbf{M} is automatically symmetric about ab and AB . Also, in the absence of the Skyrme term Eq. (7) reduces to the semilinear equation known as the classical $O(3)$ sigma model.

In what follows we will see that the energy momentum tensor plays a crucial role in the description of the propagation cones. Since the Faddeev-Niemi model can be viewed as the restriction of the Skyrme model to the “equator” of the target 3-sphere, the energy momentum tensor discussed in [27] can be directly applied to our context. In particular, $T^{ab} = T^{ab}_{(1)} + T^{ab}_{(2)}$ with

$$T^{ab}_{(1)} = L^{ab} - L^c{}_c g^{ab}/2, \\ T^{ab}_{(2)} = [F^a{}_c F^{cb} + F_{cd} F^{cd} g^{ab}/4]\kappa^2,$$

and satisfies the dominant energy condition, i.e. $T^a{}_b t^b$ is future directed for all timelike t^b . It is worth pointing out, however, that although solutions of the FN model are automatically solutions of the restricted $SU(2)$ Skyrme model, the principal symbol for the latter is given by a 3×3 matrix, which would complicate substantially the characteristic analysis performed in the next section (see [28] for some preliminary results on the hyperbolicity and instabilities for the Skyrme model).

⁴Note that Eq. (7) is equivalent to $[(h_{AB}\eta^{ab} - \kappa^2\epsilon_{AB}F^{ab})\partial_b\phi^B]_{||C}\partial_a\phi^C = 0$.

III. CHARACTERISTIC SURFACES

The nonlinear structure of the field equations implies that linearized waves interact with background solutions in a nontrivial way. The characteristic surfaces of the model can be obtained with the eikonal approximation. Formally, we consider a one-parameter family of solutions of the form

$$\phi^A(x) = \phi^A_0(x) + \alpha\varphi^A(x)\exp(i\Sigma(x)/\alpha), \quad (12)$$

where $\phi^A_0(x)$ is a smooth solution and let the real parameter $\alpha \rightarrow 0$. In this limit, we can discard all semilinear contributions in (10) and only consider the principal part term contributions.

Defining the wave covector $k_a \equiv \partial_a \Sigma$, the equation of motion reduces to the eigenvalue equation

$$[M_{AB}(\phi_0, k)]\varphi^B = 0, \quad (13)$$

where we defined the symmetric matrix $M_{AB}(\phi_0, k) \equiv M^{ab}_{AB}(\phi_0)k_a k_b$. It follows that (13) can be solved only if k_a satisfy the algebraic conditions

$$F_x(\phi_0, k) \equiv \det(M_{AB}(\phi_0, k)) = 0. \quad (14)$$

As a consequence, at a given spacetime point, the wave normals are characterized by the roots of a multivariate polynomial of fourth order⁵ in k_a in the cotangent space $T^*_p M$. The resulting algebraic variety changes from point to point in a way completely prescribed by the background solution ϕ^A_0 and the nonlinearities of the model.

The general form of F_x is given by a quartic polynomial that factorizes. In other words the characteristic polynomial reduces to a product of two simpler quadratic terms satisfying

$$[\eta^{ab}k_a k_b][(h^{-1})^{cd}k_c k_d] = 0. \quad (15)$$

Surprisingly, the reciprocal quadratic form $(h^{-1})^{ab}$ can be written in terms of the total energy momentum tensor of the background field

$$(h^{-1})^{ab} \equiv (1 - \kappa^2 \mathcal{L})\eta^{ab} + \kappa^2 T^{ab}, \quad (16)$$

where \mathcal{L} is nothing but the Lagrangian of the model and $T^{ab} = T^{ab}_{(1)} + T^{ab}_{(2)}$. As a consequence, the vanishing sets of (15) constitute the FN analogues of the Fresnel equation encountered in optics. They play the role of a fourth order spacetime dispersion relation (at least up to a conformal factor). In general, $\Sigma(x)$ will solve one quadratic polynomial or the other, although it is possible that there exist some directions where the vanishing sets coincide. Consequently, the model admits two different types of

⁵A similar calculation for the $SU(2)$ Skyrme model leads to a sixth order polynomial.

waves. One wave travels with the velocity of light while the other travels with a velocity which depends implicitly on the solution and on the Hopf charge. More explicitly, we have

$$(h^{-1})^{ab} = (1 - 2\kappa^2 \mathcal{L})\eta^{ab} + \kappa^2(L^{ab} + \kappa^2 F^a_c F^{cb}) \quad (17)$$

which reveals that both pulled-back tensors contribute to the causal structure. Note that if κ is set to zero the FN model reduces to the usual $O(3)$ sigma model (wave map equation) implying that the effective metric becomes flat everywhere.

Now, if the quantity $(h^{-1})^{ab}$ is nondegenerate it is possible to define its inverse h_{ab} such that $(h^{-1})^{ac}h_{cb} = \delta^a_b$. In general, the *effective metric* h_{ab} defines a Lorentzian metric on spacetime, the null cones of which are the effective “sound cones” of the theory. The ray vectors q^a associated to the wave fronts are the vanishing sets of the dual polynomial G_x :

$$G_x(\phi_0, q) \equiv [\eta_{ab}q^a q^b][h_{ab}q^a q^b] = 0. \quad (18)$$

As is well known, these cones completely determine the causal structure of the theory once a solution is given. In particular, nontrivial excitations propagate along geodesics of the effective spacetime. In fact, we obtain (see, for instance, [29])

$$(h^{-1})^{ab}k_{c;a}k_b = 0, \quad (19)$$

where ; is such that $h_{ab;c} = 0$. Note that for an arbitrary solution ϕ_0 endowed with invariant Q the quadratic form h is generally curved, implying that we can use appropriate geometrical methods to describe the causal structure.

IV. QUALITATIVE ANALYSIS

We now discuss some general properties of the effective metric. For the sake of simplicity, let us suppose that the solution ϕ_0^A describes a static Hopf soliton with a given topological invariant Q . Time-dependent configurations may be easily obtained using the same framework. In the static regime Eq. (17) reduces to

$$(h^{-1})^{ab}(\vec{r}) = \begin{pmatrix} (h^{-1})^{00} & 0 \\ 0 & (h^{-1})^{ij} \end{pmatrix}$$

with \vec{r} the position vector in \mathbb{R}^3 and $i, j = 1, 2, 3$. As the field tends to its vacuum in spatial infinity, i.e. $\phi^A|_{\infty} \rightarrow \text{const}$, we automatically have $(h^{-1})^{ab}|_{\infty} \rightarrow \eta^{ab}$ which means that the effective geometry is static and asymptotically flat for all possible static solitons. This is an expected result since the solitons are supposed to be localized field structures in space with finite energy.

We now ask the following: locally, how does a wave propagate in the direction of B^a ? In other words, what is the

velocity of a disturbance evolving in the direction defined by a preimage curve at a spacetime point p ? To find this velocity, first note that the vector B^a is automatically an eigenvector of the linear operator L^a_b with a null eigenvalue. Indeed, in the static regime we have

$$L^a_b t^b = 0, \quad L^a_b B^b = 0, \quad (20)$$

meaning that the kernel of L^a_b is determined by a timelike vector t^a and the magnetic field itself. A direct inspection in Eq. (1) implies that the projection $F^a_c F^c_b B^b$ also vanishes. Now, the wave front is determined by a covector $k_a \in T_p^*M$ of the form $k_a = r t_a + s B_a$ with (r,s) real components. Using the above results in Eq. (17) it follows directly

$$(h^{-1})^{ab}k_a k_b = 0 \rightarrow \eta^{ab}k_a k_b = 0. \quad (21)$$

Thus, the vector field B^a defines special directions where the effective cone coincides with the Minkowski cone. In other words, the preimages of the map ϕ^A in \mathbb{R}^3 define directions where the effective causal structure is not affected by the solution. Note, however, that because the preimage curves are linked in a nontrivial way, the resulting light cones in the global may have a very complicated structure.

What about wave propagation in other directions? Following Manton [25] we suppose that L_{ab} can be diagonalized relative to η_{ab} in a given spacetime point p . As is well known the eigenvalues are necessarily nonnegative and due to rank considerations two of them vanish identically. Choosing the spatial axis in such a way that $B_a = (0, 0, 0, B_3)$ it follows

$$L_{ab} = \text{diag}(0, \lambda_1^2, \lambda_2^2, 0), \\ F^a_c F^{cb} = \text{diag}(0, \lambda_1^2 \lambda_2^2, \lambda_1^2 \lambda_2^2, 0).$$

In particular, we have $B^a B_a = -\lambda_1^2 \lambda_2^2$. Using Eq. (22) in Eq. (17) leads to an automatically diagonal $(h^{-1})^{ab}$:

$$(h^{-1})^{00} = +(1 + \kappa^2 \lambda_1^2)(1 + \kappa^2 \lambda_2^2), \\ (h^{-1})^{11} = -(1 + \kappa^2 \lambda_2^2), \\ (h^{-1})^{22} = -(1 + \kappa^2 \lambda_1^2), \\ (h^{-1})^{33} = -(1 + \kappa^2 \lambda_1^2)(1 + \kappa^2 \lambda_2^2).$$

Two important results emerge: (i) The effective metric has a Lorentzian signature $(+---)$ for all possible static solitons.⁶ This means that the linearization of the equations of motion (9) on top of a static solution yields a well-defined causal structure. (ii) Wave propagation is always subluminal, implying that the theory is causal. In particular, velocities of propagation orthogonal to the preimage curve

⁶At least when the quantities λ_i are sufficiently regular everywhere.

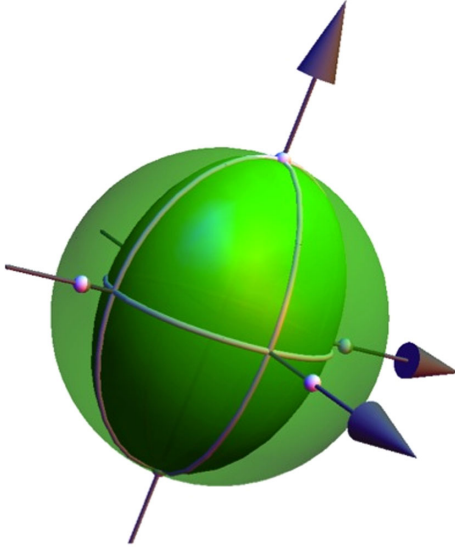


FIG. 2 (color online). Cross section of the effective “light” cone in $T_p M$. The round sphere represents velocities of propagation according with the Minkowski metric. Note that they intersect in the direction of B^a .

are of the form $c_i^2 = (1 + \kappa^2 \lambda_i^2)^{-1}$ with $i = 1, 2$. Note that they tend to 1 in spatial infinity.

The “sound” cones of the theory may be obtained also in terms of the null intervals,

$$(dx_0)^2 - (1 + \kappa^2 \lambda_1^2)(dx_1)^2 - (1 + \kappa^2 \lambda_2^2)(dx_2)^2 - dx_3^2 = 0. \quad (22)$$

It follows that, locally, the cross sections of the effective cone in the tangent space are described by ellipsoids with major axis oriented in the directions defined by B^a . This result is valid for all possible preimages $\phi^A = \text{const}$ for all possible charges. See Fig. 2 for an illustration. Again, we stress that because links between preimages are nontrivial and eigenvalues are space-dependent quantities there will be a highly complex causal structure associated. It remains the possibility that linked or knotted congruences of rays emerge in \mathbb{R}^3 with regions where waves are trapped.

V. RATIONAL MAPS AND APPROXIMATE EFFECTIVE GEOMETRIES

In this section we use the rational map *ansatz* introduced by Suttcliffe in [17] (see also [30]) in order to explore approximate expressions for $(h^{-1})^{ab}$. The idea is to achieve a qualitative picture of the metrics without appealing to complicated numerical simulations.

The strategy is as follows. Recall that the assumption $\phi^A|_\infty = \text{const}$ effectively compactifies \mathbb{R}^3 to the hypersphere \mathbb{S}^3 . A point of \mathbb{S}^3 can be thought also as a point of the plane of complex dimension 2 with coordinates (Z_1, Z_0) and $|Z_1|^2 + |Z_0|^2 = 1$. Project the point (Z_1, Z_0) onto \mathbb{R}^3 using the map

$$(Z_1, Z_0) = \left(\frac{x_1 + ix_2}{r} \sin f, \cos f + i \frac{\sin f}{r} x_3 \right), \quad (23)$$

where (x_1, x_2, x_3) are Cartesian coordinates, $r = (x_1^2 + x_2^2 + x_3^2)^{1/2}$ and $f(r)$ is a monotonically decreasing function such that $f(0) = \pi$ and $f(\infty) = 0$. Interpret \mathbb{S}^2 as a Riemann sphere introducing a complex coordinate W . The idea is to start with spherical coordinates $\phi^A = (\Theta, \Phi)$ and metric $h_{AB} = \text{diag}(1, \sin^2 \Theta)$. Then, do a stereographic projection from the south pole \mathbf{S} ($\Theta = \pi$) to the equatorial plane to obtain $W = R e^{i\Phi}$ with the absolute value given by $R = \tan(\Theta/2)$. Finally, write W as a rational function of the complex quantities Z_1 and Z_0 in the form

$$W = p(Z_1, Z_0)/q(Z_1, Z_0) \quad (24)$$

where p and q are polynomials.

As a consequence, for each point $W \in \mathbb{S}^2$, we obtain a closed curve $\phi^{-1}(W)$ in \mathbb{R}^3 , whose image by ϕ^A is the point W .⁷ The tangent vectors to these curves define precisely the direction of B^a . In particular, we can obtain the whole of the \mathbb{R}^3 as “fibers” over the ordinary 2-sphere. Incidentally, for any two points, W_1 and W_2 on \mathbb{S}^2 , the corresponding fibers are nontrivially linked. The number of links depends crucially on the degree of the polynomials $p(Z_1, Z_0)$ and $q(Z_1, Z_0)$.

The point here is that once p and q are given as functions of Z_1 and Z_0 , the effective metric may be easily obtained. This can be accomplished writing the pull-back quantities L_{ab} and F_{ab} in terms of the derivatives of W . We obtain

$$L_{ab} = \frac{2}{(1 + |W|^2)^2} \partial_{(a} W \partial_{b)} \bar{W}, \quad (25)$$

$$F_{ab} = \frac{2i}{(1 + |W|^2)^2} \partial_{[a} W \partial_{b]} \bar{W}, \quad (26)$$

with $(a, b) = (ab + ba)$ and $[a, b] = ab - ba$ and \bar{W} the complex conjugate.⁸ Basically, there will be three different classes of effective geometries. They follow naturally from the classification presented in [17] for all possible background fields. Roughly, they describe the causal structures associated to

- (1) Toroidal fields $\mathcal{A}_{n,m}$: $W = Z_1^n / Z_0^m$, with $n, m \in \mathbb{Z}$ and $Q = n.m$;

⁷It is also common to call the preimage as the “fiber” over the point W .

⁸Alternatively, we have

$$L_{ij} = \frac{4}{(1 + R^2)^2} (\partial_i R \partial_j R + R^2 \partial_i \Phi \partial_j \Phi),$$

$$F_{ij} = \frac{4}{(1 + R^2)^2} \partial_{[i} R \partial_{j]} \Phi.$$

- (2) (a,b)-torus knots \mathcal{K}_{ab} : $W = Z_1^\alpha Z_0^\beta / (Z_1^a + Z_1^b)$, with α a positive integer, β a non-negative integer and a, b coprime positive integers with $a > b$ and $Q = ab + \beta a$;
- (3) Linked Hopfions $\mathcal{L}_{p,q}^{\alpha,\beta}$: $W = Z_1^\alpha Z_0^\beta / (Z_1^p + Z_1^q)$ with α a positive integer, β a non-negative integer p, q not coprime.

As a consequence of the above *ansatz*, one is now able to speak about effective geometries engendered by knotted structures. Each geometry carries implicitly a Hopf charge with it and is somehow related to the homotopy class of the configuration. Waves are described by pencils of null geodesics scattered by the corresponding geometry and it is possible that they remain trapped for some regions of the effective spacetime. In order to understand better these aspects, it would be interesting to analyze in more detail the geometrical and topological properties of the above metrics, including their symmetries (see [31] for a Bianchi classification in the helical phase of chiral nematic liquid crystals). In particular, one could investigate the approximate behavior of geodesics arriving from the vacuum and scattered by the solitonic structure. We shall come back to these questions in the future.

A. Example: $Q = 1$ Hopfion

As a final remark, let us illustrate the qualitative behavior of the preimages in \mathbb{R}^3 for the $Q = 1$ Hopfion. As discussed above, they define directions where the waves “perceive” the actual Minkowski spacetime. In other words, metrical relations are only distorted for intervals having some component orthogonal to B^a .

In this case the rational map is simply $W = Z_1/Z_0$. For the sake of simplicity we choose a profile function with an exponential decay of the form $f(r) \equiv \pi e^{-r^2}$. We can now calculate the absolute value (R) and the argument (Φ) as explicit functions of the coordinates (x_1, x_2, x_3) . Now, instead of only considering preimages of points, we will consider preimages of whole sets on \mathbb{S}^2 . In particular, we consider the preimages of the parallels $R = \text{const}$ and the meridians $\Phi = \text{const}$. They characterize two families of surfaces in \mathbb{R}^3 . Surfaces with constant R are homeomorphic to tori. The tori are nested, and their size increase as R decreases. In particular, one obtains a one-dimensional curve in the limit $R \rightarrow \infty$. This curve is precisely the position of the Hopfion. Surfaces with constant Φ are not so simple. They are homeomorphic to parabolic Dupin cyclides, i.e. a specific inversion of the torus.

The points where a parallel intersects a meridian in \mathbb{S}^2 are given by the intersections of $\phi^{-1}(R = \text{const})$ and $\phi^{-1}(\Phi = \text{const})$ in \mathbb{R}^3 . They are closed curves pairwise linked. We can see such a general behavior in Fig. 3. The figure shows the intersection between the meridian $\Phi = 0$ and a parallel $R = 1$. Now, if we consider the collection of all points lying in \mathbb{S}^2 we obtain the congruence of magnetic field lines filling the entire space (see Fig. 4). They can be

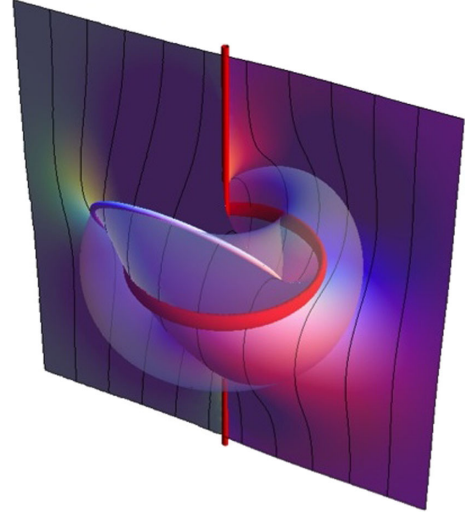


FIG. 3 (color online). Intersection of a torus and a parabolic Dupin cyclide. The resulting closed curve is the preimage of a point in the unit sphere where a parallel meets a meridian. The figure shows also the position of the Hopfion and the preimage of infinity.

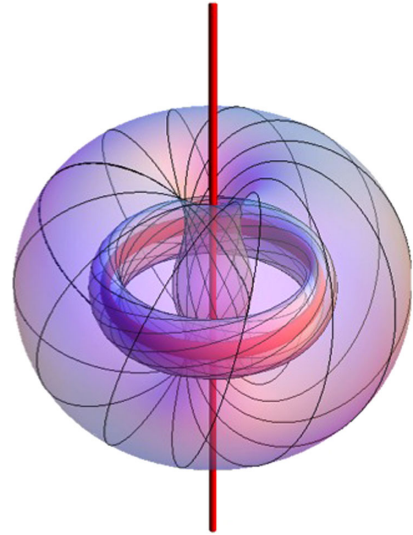


FIG. 4 (color online). Global behavior of the magnetic field lines. Metrical relations remain the same in the directions of the fibers while they are distorted in any other direction.

thought as a continuous deformation of the usual Hopf fibration [32]. Roughly, effective metrical relations are the same in the directions of the fibers while they are distorted in any other direction, leading to a nontrivial causal structure in the global.

ACKNOWLEDGMENTS

E. Goulart would like to thank CAPES–Brazil process No. 2383136 for financial support and G. W. Gibbons for comments and suggestions.

- [1] N. S. Manton and P. Sutcliffe, *Topological Solitons* (Cambridge University Press, Cambridge, England, 2004).
- [2] Y. Kawaguchi, M. Nitta, and M. Ueda, Knots in a Spinor Bose-Einstein Condensate, *Phys. Rev. Lett.* **100**, 180403 (2008).
- [3] P. Sutcliffe, Vortex rings in ferromagnets: Numerical simulations of the time-dependent three-dimensional Landau-Lifshitz equation, *Phys. Rev. B* **76**, 184439 (2007).
- [4] A. M. Kamchatnov, Topological solitons in magnetohydrodynamics, *Sov. Phys. JETP* **55**, 69 (1982).
- [5] L. D. Faddeev and A. J. Niemi, Knots and particles, *Nature (London)* **387**, 58 (1997).
- [6] T. Machon and G. P. Alexander, Knots and nonorientable surfaces in chiral nematics, *Proc. Natl. Acad. Sci. U.S.A.* **110**, 14174 (2013).
- [7] R. Slobodeanu, Steady Euler flows and the Faddeev-Niemi model with mass term, [arXiv:1405.3469](#).
- [8] T. H. R. Skyrme, *Proc. R. Soc. A* **260**, 127 (1961); G. E. Brown and M. Rho, *The Multifaceted Skyrmion* (World Scientific Publishing, Singapore, 2010).
- [9] S. V. Shabanov, An effective action for monopoles and knot solitons in Yang-Mills theory, *Phys. Lett. B* **458**, 322 (1999).
- [10] Y. M. Cho, Monopoles and Knots in Skyrme Theory, *Phys. Rev. Lett.* **87**, 252001 (2001).
- [11] L. D. Faddeev and A. J. Niemi, Aspects of electric magnetic duality in SU(2) Yang-Mills theory, *Phys. Lett. B* **525**, 195 (2002).
- [12] A. J. Niemi, International Symposium on Color Confinement and Hadrons in Quantum Chromodynamics—Confinement 2003, Wako, Japan, 2003, [arXiv:hep-th/0312133](#).
- [13] F. D. Faddeev and A. J. Niemi, Spin-charge separation, conformal covariance and the SU(2) Yang-Mills Theory, *Nucl. Phys. B* **776**, 38 (2007).
- [14] R. A. Battye and P. M. Sutcliffe, To be or Knot to be?, *Phys. Rev. Lett.* **81**, 4798 (1998).
- [15] R. A. Battye and P. M. Sutcliffe, Solitons, links and knots, *Proc. R. Soc. A* **455**, 4305 (1999).
- [16] J. Hietarinta and P. Salo, Faddeev-Hopf knots: Dynamics of linked un-knots, *Phys. Lett. B* **451**, 60 (1999).
- [17] P. Sutcliffe, Knots in the Skyrme-Faddeev model, *Proc. R. Soc. A* **463**, 3001 (2007).
- [18] J. Shatah, Weak solutions and development of singularities of the SU(2) σ -Model, *Commun. Pure Appl. Math.* **41**, 459 (1988).
- [19] W. Wai-Yeung Wong, Regular hyperbolicity, dominant energy condition and causality for Lagrangian theory of maps, *Classical Quantum Gravity* **28**, 215008 (2011).
- [20] D. Tataru, Wave maps, *Bull. Am. Math. Soc.* **41**, 185 (2004).
- [21] E. Goulart and S. E. Perez Bergliaffa, Effective metric in nonlinear scalar field theories, *Phys. Rev. D* **84**, 105027 (2011).
- [22] C. Barcelo, S. Liberati, and M. Visser, Analogue gravity, *Living Rev. Relativity* **8**, 12 (2005).
- [23] D. Christodoulou, *The Formation of Shocks in 3-dimensional Fluids* (European Mathematical Society, Zurich, 2007).
- [24] G. W. Gibbons and E. Goulart, Inspecting baby-Skyrmions with effective metrics, *Phys. Rev. D* **89**, 105008 (2014).
- [25] N. S. Manton, *Commun. Math. Phys.* **111**, 469 (1987).
- [26] J. H. C. Whitehead, An expression of Hopf's invariant as an integral, *Proc. Natl. Acad. Sci. U.S.A.* **33**, 117 (1947).
- [27] G. W. Gibbons, Causality and the Skyrme model, *Phys. Lett. B* **566**, 171 (2003).
- [28] W. Y. Crutchfield and J. B. Bell, Instabilities of the Skyrme model, *J. Comput. Phys.* **110**, 234 (1994).
- [29] M. Novello, V. A. De Lorenci, J. M. Salim, and R. Klippert, *Phys. Rev. D* **61**, 045001 (2000); M. Visser, C. Barcelo, and S. Liberati, in *Inquiring the Universe*, Frontier Group, [arXiv:gr-qc/0204017](#).
- [30] R. A. Battye and M. Haberichter, Classically isospinning Hopf solitons, *Phys. Rev. D* **87**, 105003 (2013).
- [31] G. W. Gibbons and C. M. Warnick, The helical phase of chiral nematic liquid crystals as the Bianchi VII(0) group manifold, *Phys. Rev. E* **84**, 031709 (2011).
- [32] H. K. Urbantke, The Hopf fibration—seven times in physics, *J. Geom. Phys.* **46**, 125 (2003).